mAbs

ISSN: 1942-0862 (Print) 1942-0870 (Online) Journal homepage: www.tandfonline.com/journals/kmab20

# Design and preclinical characterization of an affinity-tuned BCMA×CD3 bispecific T-cell engager for broad B-cell depletion

**Jamie Thomas , Gang Xu , Hannah Lock , Qin Song , Yumei Yin , Wanying Luo , Kyu Hong , Liguang Lou , Changyu Wang , Leslie Chinn , Neelufar Mozaffarian , Jaideep Dudani , Paul Bessette , Charlie Zhou , Ruth Lan , Bo Chen & Nishant Mehta**

**To cite this article:** Jamie Thomas , Gang Xu , Hannah Lock , Qin Song , Yumei Yin , Wanying Luo , Kyu Hong , Liguang Lou , Changyu Wang , Leslie Chinn , Neelufar Mozaffarian , Jaideep Dudani , Paul Bessette , Charlie Zhou , Ruth Lan , Bo Chen & Nishant Mehta (2026) Design and preclinical characterization of an affinity-tuned BCMA×CD3 bispecific T-cell engager for broad B-cell depletion, mAbs, 18:1, 2718587, DOI: 10.1080/19420862.2026.2718587

**To link to this article:** https://doi.org/10.1080/19420862.2026.2718587

MABS
2026, VOL. 18, NO. 1, 2718587
https://doi.org/10.1080/19420862.2026.2718587

Taylor & Francis
by informa

REPORT

OPEN ACCESS Check for updates

# Design and preclinical characterization of an affinity-tuned BCMA×CD3 bispecific T-cell engager for broad B-cell depletion

Jamie Thomas[a*], Gang Xu[b*], Hannah Lock[a*], Qin Song[b], Yumei Yin[b], Wanying Luo[b], Kyu Hong[a], Liguang Lou[c], Changyu Wang[b], Leslie Chinn[a], Neelufar Mozaffarian[a], Jaideep Dudani[a], Paul Bessette[a], Charlie Zhou[a], Ruth Lan[a], Bo Chen[b], and Nishant Mehta[a]

[a]Ouro Medicines, South San Francisco, CA, USA; [b]Keymed Biosciences, Chengdu, China; [c]Shanghai Institute of Materia Medica, Chinese Academy of Sciences, Shanghai, China

**ABSTRACT**

B cell maturation antigen (BCMA) is a validated target for plasma cell depletion; however, T cell–redirecting approaches must balance potent cytotoxicity with controlled T cell activation. Here, we describe the design and preclinical characterization of gamgertamig, an affinity-tuned BCMA×CD3 bispecific T-cell engager engineered to promote target-dependent activity. Gamgertamig is a humanized IgG4-based 1 + 1 bispecific antibody incorporating Fc-silencing mutations and a reduced-affinity CD3-binding arm, resulting in a >50-fold affinity bias toward BCMA relative to CD3. Gamgertamig exhibited high-affinity binding to BCMA and mediated potent, antigen-dependent cytotoxicity across B cell and myeloma cell lines spanning a wide range of target densities, with sub-nanomolar $EC_{50}$ values. In primary human peripheral blood mononuclear cells (PBMCs), gamgertamig induced robust depletion across B cell subsets, including naïve, memory, and transitional populations. Consistent activity was observed across samples from healthy donors and patients with autoimmune diseases and multiple myeloma. In vivo, gamgertamig produced dose-dependent tumor inhibition in human PBMC-reconstituted xenograft models and sustained depletion of circulating B cells and bone marrow plasma cells in rhesus monkeys, with a serum half-life exceeding five days. Together, these data demonstrate that gamgertamig mediates potent, target-dependent cytotoxicity and broad depletion of disease-relevant B-cell populations, supporting its development as a BCMA×CD3 T-cell engager for autoimmune diseases and B-cell malignancies.

**ARTICLE HISTORY**
Received 27 April 2026
Revised 8 July 2026
Accepted 13 July 2026

**KEYWORDS**
Affinity-tuned; autoimmunity; BCMA; bispecific antibody; immune reset; T-cell engager

## Introduction

B cell-depleting or modulating therapies are extensively validated in the treatment of autoimmune diseases, including indications such as rheumatoid arthritis (RA) and systemic lupus erythematosus (SLE).[1,2] Recent clinical data demonstrate that B cell depleting therapies using potent mechanisms of action, such as chimeric antigen receptor T (CAR-T) cells[3] and T-cell engagers (TCE),[4] can induce immune "reset."[5] Immune reset is defined by the elimination of both the autoantibody-producing plasma cells and the autoreactive memory compartments, followed by reconstitution with a naïve immune system, resulting in durable clinical remissions off therapy. Recent trials with CD19 CAR-T cells have shown remarkable efficacy in relapsed or refractory autoimmune disease with immune reset in some indications.[3] However, CD19- and CD20-directed therapies are unable to eliminate terminally differentiated plasma cells, which often lack these surface markers.[6–8] The persistence of these autoreactive plasma cells following CD19 CAR-T therapy is hypothesized to be a key driver of non-response and disease relapse, and may be clinically relevant in indications that are primarily plasma cell-driven, including Sjögren's disease (SjD), immune thrombocytopenia (ITP), autoimmune hemolytic anemia, and idiopathic inflammatory myopathies.[4,9–11]

**CONTACT** Bo Chen bochen@keymedbio.com Keymed Biosciences, Chengdu, China; Nishant Mehta nmehta@ouromeds.com Ouro Medicines, South San Francisco, CA, USA

*These authors contributed equally.

Supplemental data for this article can be accessed online at https://doi.org/10.1080/19420862.2026.2718587

B cell maturation antigen (BCMA) is a member of the tumor necrosis factor receptor (TNFR) superfamily that is highly expressed on plasmablasts and long-lived plasma cells (LLPC), which sustain long-term autoantibody production.[12] Its ligands, APRIL and BAFF, engage BCMA and TACI to activate NF-κB and PI3K survival pathways in plasma cells.[12,13] Emerging evidence indicates that BCMA expression extends into earlier $CD19^+$ B cell subsets, including the memory compartment, which are also deeply depleted by potent therapeutic modalities targeting BCMA.[14,15] Levels of BCMA on earlier $CD19^+$ B cells are substantially lower than on plasma cells and may be difficult to detect by conventional flow cytometry, but emerging clinical and high-sensitivity profiling studies suggest that they can be sufficient for depletion by potent BCMA-directed therapies. Eliminating $BCMA^+$ plasma cells and earlier lineage B cells therefore represents a rational strategy to suppress autoantibody production, achieve durable disease control and potentially achieve immune reset.

Bispecific TCEs, which facilitate a non-T cell receptor-restricted immune synapse between cytotoxic T cells and target antigen-expressing cells, have emerged as an effective modality for B cell/plasma-cell depletion. BCMA-directed TCEs have demonstrated robust clinical activity in relapsed/refractory multiple myeloma,[16] and clinical data suggest feasibility for the treatment of autoimmune diseases.[4] While CAR-T therapies can also induce deep and durable responses via B cell depletion, TCEs offer advantages in scalability and manufacturing, avoid the need for lymphodepleting preconditioning, and allow for step-up dosing strategies to mitigate cytokine-release syndrome and other adverse reactions.

A central challenge in the development of T cell–redirecting bispecific antibodies is achieving potent target-cell killing while controlling T-cell activation and cytokine release. Herein, we describe the development of gamgertamig, a BCMA×CD3 bispecific TCE designed to deplete BCMA-expressing B-lineage and plasma-cell populations relevant to autoimmune disease and B cell malignancies. Gamgertamig incorporates an Fc-silenced antibody format to preserve the pharmacokinetic (PK) advantages of FcRn interaction while minimizing Fc-mediated effector function, together with a reduced-affinity CD3-binding arm intended to support target-dependent T-cell engagement. In vitro, gamgertamig mediates potent cytotoxicity across early and late B-lineage populations in peripheral blood mononuclear cells (PBMCs) from healthy donors and patients with autoimmune disease. In vivo, gamgertamig demonstrates robust activity in $BCMA^+$ tumor xenografts in humanized mice and induces sustained depletion of B cell and plasma-cell compartments in nonhuman primate studies.

## Results

### *Gamgertamig design and molecular properties*

Gamgertamig is a humanized, bispecific, 1 + 1 TCE antibody with an IgG-like format. A knobs-into-holes heterodimerization strategy using a human IgG4 isotype backbone was used to pair BCMA- and CD3ε-specific Fab domains (Figure 1A). The stabilizing hinge mutation S228P was incorporated to minimize Fab-arm exchange, and Fc-silencing substitutions L235E and P329A were introduced to abrogate Fcγ receptor- and complement-mediated effector functions while preserving FcRn binding for half-life extension. To promote cognate heavy- and light-chain pairing, paired charge mutations were introduced within the variable-domain framework regions of both antigen-binding arms. Specifically, the BCMA-binding arm contains Gln42Lys in the variable light (VL) chain and Gln39Glu in the variable heavy (VH) chain, whereas the CD3ε-binding arm contains Gln40Glu in VL and Gln39Lys in VH. These substitutions were incorporated to favor electrostatic complementarity within the intended VH/VL pairs and reduce non-cognate light-chain pairing.[17]

The CD3-binding arm was derived from a murine anti-CD3 antibody of the SP34 lineage and humanized by grafting complementarity-determining regions onto human germline framework regions (IGHV3/IGLV7 families). To preserve binding while increasing human sequence content, multiple humanized variants incorporating limited framework substitutions were generated. Combinatorial pairing of these heavy- and light-chain variants produced a panel of CD3 VH/VL combinations, which were screened for binding to CD3-expressing Jurkat cells (Figure 1B). A variant comprising the hVH9 and hVL5 domains was selected that retained CD3 binding but exhibited reduced cellular engagement relative to higher-affinity variants. This intermediate-binding CD3 arm was prioritized to enable controlled T cell engagement and to support target-dependent activation in the bispecific format.

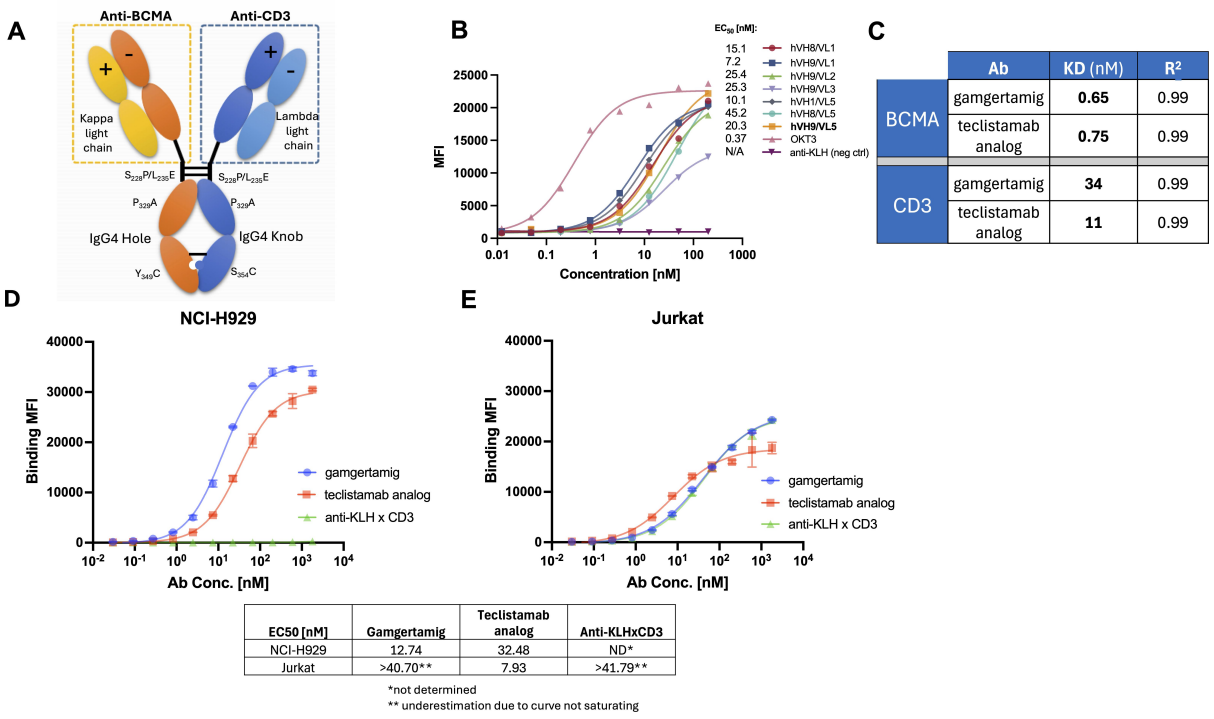


| EC50 [nM] | Gamgertamig | Teclistamab analog | Anti-KLHxCD3 |
|---|---|---|---|
| NCI-H929 | 12.74 | 32.48 | ND* |
| Jurkat | >40.70** | 7.93 | >41.79** |

*not determined
** underestimation due to curve not saturating

**Figure 1.** Gamgertamig structure and binding properties. (A) Schematic representation of gamgertamig showing the IgG-like 1+1 bispecific format and knobs-into-holes heterodimerization strategy, with indicated Fc and variable domain mutations. (B) Screening of humanized CD3 VH/VL variants for binding to CD3-expressing Jurkat cells. Binding was assessed by flow cytometry, and a variant comprising hVH9/hVL5 was selected based on retention of binding with reduced cellular engagement relative to higher-binding variants. (C) Bio-layer interferometry (BLI) analysis of binding affinity of gamgertamig and a teclistamab analog to recombinant human BCMA and CD3. Both molecules exhibit high-affinity binding to BCMA, while gamgertamig shows reduced affinity for CD3. (D) Cell-based binding of gamgertamig, teclistamab analog, and a CD3 T cell engager control to BCMA-expressing NCI-H929 cells, measured by flow cytometry. (E) Cell-based binding of gamgertamig, teclistamab analog, and a CD3 T cell engager control to CD3-expressing Jurkat cells. Binding did not reach saturation at the highest concentrations tested for gamgertamig and CD3 control, and therefore calculated $EC_{50}$ values likely underestimate the true equilibrium binding constant.

The BCMA-binding arm was isolated from a mouse-derived immune phage-display library using recombinant BCMA and subsequently humanized, yielding a high-affinity clone with robust cross-reactivity to human and non-human primate orthologs. Following humanization, two light-chain and two heavy-chain sequence variants were generated and combinatorially paired to produce a panel of four BCMA×CD3 bispecific constructs (κλ003–κλ006), all incorporating a common set of charge-pairing mutations and the same CD3-binding arm. Across this panel, the molecules exhibited comparable BCMA binding affinity and cellular activity, indicating that these sequence variations did not materially alter target engagement (Supplementary Figure S1). A representative construct (κλ005) was advanced for further characterization and is referred to as gamgertamig in the following sections.

## *Binding to BCMA and CD3*

The binding kinetics of gamgertamig were compared to a teclistamab analog using bio-layer interferometry (BLI). Both molecules exhibited similar high-affinity binding to BCMA, with equilibrium dissociation constants ($K_d$) of 0.65 nM for gamgertamig and 0.75 nM for the teclistamab analog (Figure 1C). However, the affinity of gamgertamig for the human CD3ε/δ heterodimer was approximately 3-fold weaker than that of the teclistamab analog. As a result, gamgertamig exhibited a > 50-fold higher affinity for BCMA relative to CD3, compared to ~15-fold for the teclistamab analog. This affinity bias is consistent with the design objective of prioritizing target cell occupancy and minimizing nonspecific T cell engagement in the absence of antigen.

Binding of gamgertamig to native target proteins was evaluated using cell-based assays and compared with a teclistamab analog. Gamgertamig demonstrated dose-dependent binding to $BCMA^+$ NCI-H929 multiple myeloma cells and to $CD3^+$ Jurkat T cells (Figure 1D,E). On NCI-H929 cells, gamgertamig showed stronger apparent BCMA binding than the teclistamab analog, with $EC_{50}$ values of 12.74 nM and 32.48 nM, respectively. In contrast, on Jurkat cells, gamgertamig showed weaker apparent CD3 binding than the teclistamab analog, with $EC_{50}$ values of >40.70 nM and 7.93 nM, respectively. These cell-based binding data are consistent with BLI measurements showing higher-affinity BCMA binding and reduced CD3 affinity for gamgertamig relative to the teclistamab analog. To confirm target specificity, a monovalent anti-CD3 control incorporating the same CD3-binding arm without a BCMA-targeting domain showed no detectable binding to NCI-H929 cells while maintaining CD3 engagement on Jurkat cells.

## *Gamgertamig mediates potent BCMA-dependent cytotoxicity and minimal cytokine release in B cell lines*

To evaluate the cytotoxic potency of gamgertamig across a spectrum of antigen densities, we utilized a panel of B cell leukemia and myeloma cell lines. Surface BCMA quantification via QuantiBRITE-PE beads identified NCI-H929 as a high-expressor (25,300 receptors/cell) and Mino as a low-expressor (1,100 receptors/cell) (Figure 2A). This order-of-magnitude difference in receptor density between NCI-H929 and Mino provided a robust model to assess the sensitivity of gamgertamig-mediated T cell engagement.

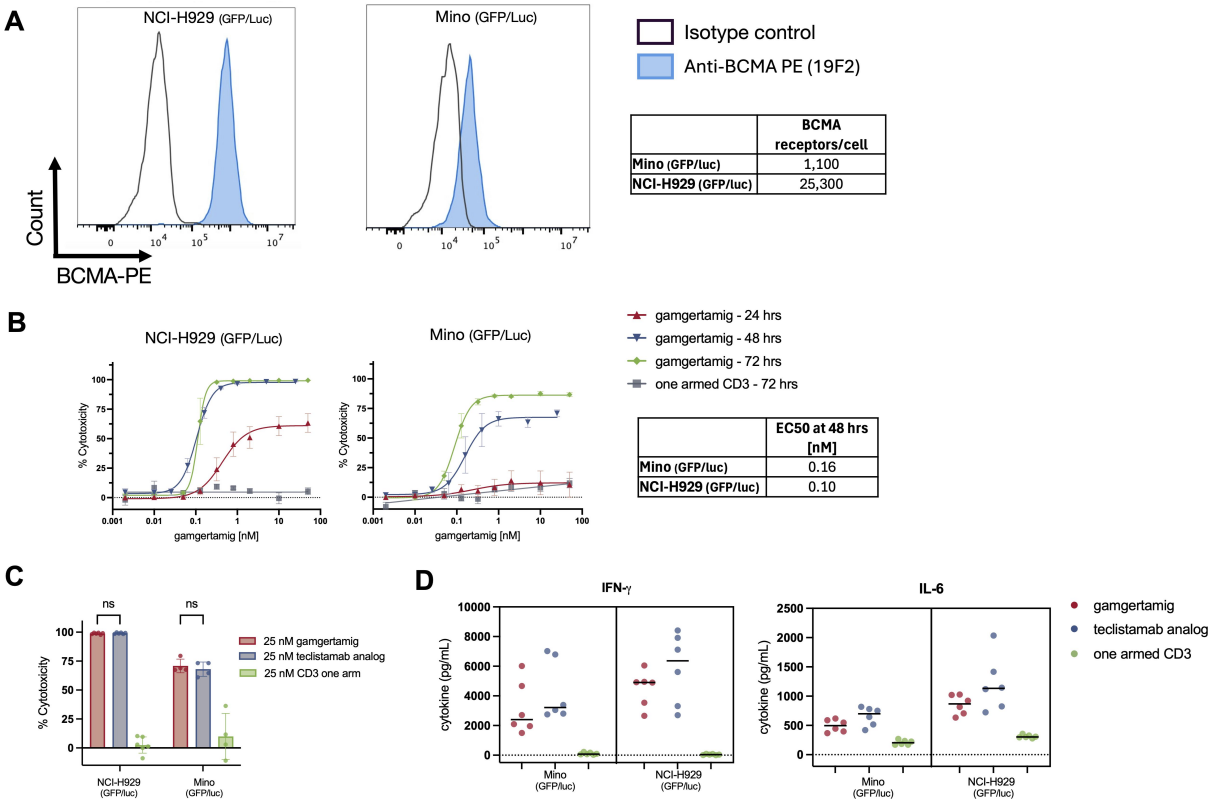


**Figure 2.** Gamgertamig induces potent cytotoxicity with limited cytokine release in BCMA-expressing cell lines. (A) Staining of NCI-H929 (GFP/luc) and Mino (GFP/luc) with an anti-BCMA flow antibody and receptor quantification using Quantbrite-PE beads. (B) Gamgertamig-induced cytotoxicity of BCMA-expressing cells across 24, 48, and 72 hours compared to cytotoxicity of a one-armed CD3 negative control using a luciferase-based plate reader assay. % Cytotoxicity was calculated by ratio of luciferase signal in treated samples compared to untreated samples. $EC_{50}$ was calculated with a non-linear agonist vs response four parameter fit via GraphPad Prism. (C) Cytotoxicity comparison at 25 nM for 48 hrs between gamgertamig, teclistamab analog, and one-armed CD3 control. (D) Cytokine release comparison at 25 nM for 48 hrs between gamgertamig, teclistamab analog, and one-armed CD3 control. Supernatant from cytotoxicity assays was measured for IFN-γ and IL-6 levels via ELISA.

Serial dilutions of gamgertamig were co-cultured with target cells and human PBMCs as effector cells at an effector-to-target (E:T) ratio of 10:1 for 24, 48, and 72 hours. Gamgertamig induced potent, BCMA-dependent lysis of both NCI-H929 and Mino cells. As expected for TCEs, maximum cytotoxicity increased at later time points, reflecting the kinetics of productive immunological synapse formation and effector expansion. This time-dependence was most pronounced in the low-BCMA-expressing Mino line, where lysis was marginal at 24 hours but exceeded 80% by 72 hours (Figure 2B). Notably, $EC_{50}$ values at 48 hours for NCI-H929 and Mino were nearly identical (0.10 nM and 0.16 nM, respectively). Minimal cytotoxicity was observed with the one-armed CD3 control at 72 hours. This result demonstrates that the potent killing observed in both cell lines was strictly dependent on the BCMA-targeting arm of gamgertamig.

Finally, we compared the cytokine release profile of gamgertamig to a teclistamab analog. At the highest concentration (25 nM) after 48 hours, both molecules achieved comparable maximal lysis, while a one-armed CD3 control showed no significant cytotoxicity (Figure 2C). To further evaluate comparative potency across the full concentration range, dose-response T cell–dependent cellular cytotoxicity (TDCC) analyses were performed with gamgertamig and the teclistamab analog in both NCI-H929 and Mino co-cultures. These analyses showed comparable maximal cytotoxicity between the two molecules, with EC50 values in the same sub-nanomolar range (Supplementary Figure S2). Analysis of co-culture supernatants revealed that gamgertamig induced numerically lower levels of IFNγ and IL-6 compared to teclistamab across Mino and NCI-H929 targets, though these trends did not reach statistical significance (Figure 2D). Full cytokine dose-response analyses similarly showed dose-dependent IFNγ and IL-6 induction for both molecules, with gamgertamig exhibiting numerically lower maximal cytokine responses than the teclistamab analog across both target-cell lines (Supplementary Figure S3).

### *Gamgertamig mediates potent, pan-B cell depletion across the entire B cell lineage*

To assess the activity of gamgertamig in a physiologically relevant context, we used an autologous co-culture system with PBMCs from healthy donors. While BCMA expression on peripheral B cells is often below the detection threshold of conventional flow cytometry, clinical experience with BCMA-directed therapies consistently shows robust peripheral B cell depletion. Additionally, peripheral B cells (including naïve, transitional, unswitched memory, switched memory, and double negative B cells) are known to express BCMA by RNAseq,[15,18] which may have greater sensitivity compared to flow cytometry. We hypothesized that trace surface expression of BCMA may be sufficient to trigger T cell–mediated cytotoxicity at the E:T ratios present in vivo.

Following 96-hour incubation, gamgertamig mediated potent, dose-dependent depletion of total $CD20^+$ B cells, reaching a maximum lysis of >75% with a mean $EC_{50}$ of 4.95 nM (Figure 3A). A monovalent CD3 control failed to induce killing, confirming that depletion is strictly dependent on bispecific antigen engagement. Characterization of B cell subsets revealed that gamgertamig activity was not restricted to late-lineage cells; instead, it mediated broad depletion across nearly the entire B cell ontogeny (Figure 3B). Naïve, unswitched memory, and switched memory B cells were all depleted with similar potency. Double-negative ($CD27^-$ $IgD^-$) and transitional ($CD24^{hi}CD38^{hi}$) B cells were the only subsets to show modestly lower maximum killing. Consistent with their low frequency in peripheral blood, plasmablasts/plasma cells were too scarce in PBMC samples to enable reliable measurement of cell killing. This pan-B cell depletion profile is consistent with emerging clinical reports of BCMA-targeting TCEs in patients with autoimmune disease, where near-total loss of peripheral $CD19^+$ B cells is observed.[10,19]

Importantly, a one-armed CD3 control lacking the BCMA-binding arm did not mediate appreciable B cell depletion, supporting a requirement for BCMA engagement despite low or undetectable surface BCMA levels on some primary B cell subsets. To further confirm BCMA-dependent B cell depletion, we performed blocking studies using healthy donor PBMCs pre-incubated with an effector-null anti-BCMA antibody containing the same BCMA-binding arm as gamgertamig but lacking a CD3-binding arm (Supplementary Figure S4). Pre-binding with anti-BCMA antibody significantly blocked B cell lysis mediated by gamgertamig at 100 nM and 20 nM, whereas an anti-CD19 control antibody did not significantly affect gamgertamig-mediated lysis. These findings further support that depletion of primary $CD20^+$ B cells is mediated through BCMA-dependent target engagement despite low or undetectable surface BCMA levels by conventional flow cytometry.

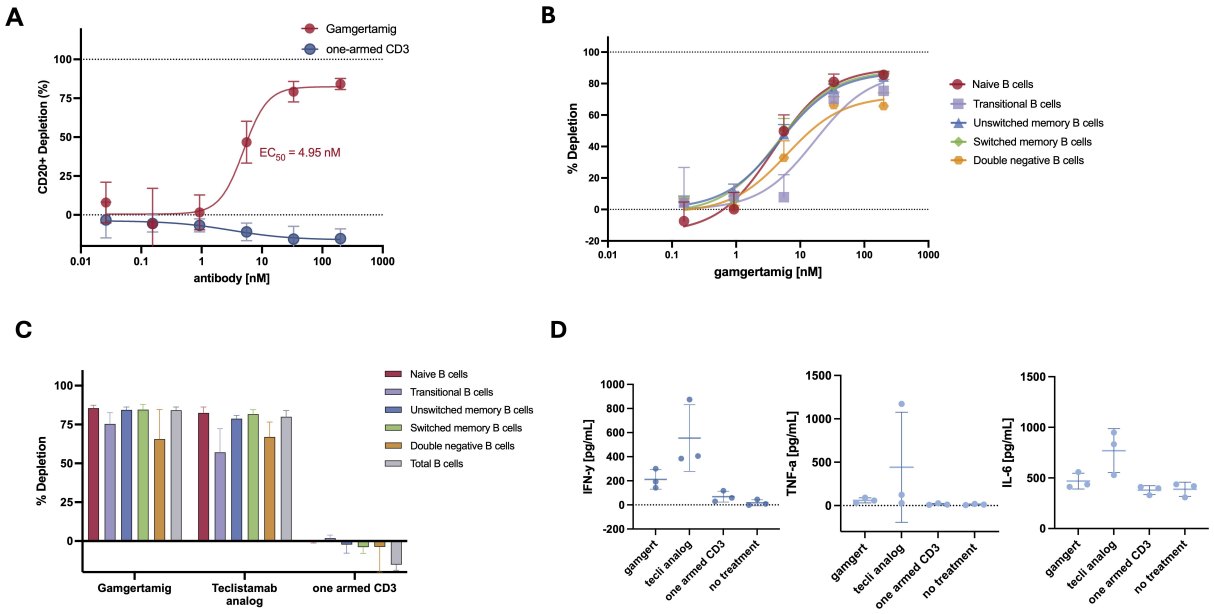


**Figure 3.** Gamgertamig induces broad B cell depletion with limited cytokine release in healthy donor PBMCs. Cytotoxicity and cytokine release were measured after a 96-hour co-culture of test articles and three healthy PBMC donors. Live $CD20^+$B cells and B cell subsets were counted via flow cytometry. Cytotoxicity (% depletion) was calculated using the ratio of live $CD3^-CD20^+$B cells or respective B cell subset in treated samples versus counts from untreated samples. Data from three healthy donors were averaged. (A) Cytotoxicity of total $CD20^+$B cells. EC50 curve was calculated with a non-linear agonist vs response four parameter fit via GraphPad Prism. (B) Depletion of individual B cell subsets. (C) The depletion of B cell subsets at the top concentration of 200 nM was compared among gamgertamig, teclistamab analog, and a one-armed CD3 negative control. Depletion of all subsets at the top concentration was similar between gamgertamig and the teclistamab analog. (D) Secreted IFN-γ, TNF-α, and IL-6 cytokines were measured via ELISA from supernatant collected after 96 hours of co-culture.

Finally, we compared gamgertamig against a teclistamab analog at a saturating concentration of 200 nM (Figure 3C). No significant differences in the depth of depletion were observed across subsets in these healthy donor samples. Notably, gamgertamig was associated with numerically lower levels of the pro-inflammatory cytokines IFNγ, TNFα, and IL-6 compared to the teclistamab analog (Figure 3D). While these differences did not reach statistical significance in this cohort, the trend toward reduced cytokine induction despite equivalent cytotoxic efficacy highlights a potentially favorable pharmacological profile that may minimize the risk of inflammatory adverse events during B cell-directed therapy.

## *Gamgertamig demonstrates consistent, potent B cell depletion across a broad range of autoimmune indications*

To evaluate whether disease-associated physiological changes might alter therapeutic efficacy, we investigated gamgertamig-mediated depletion and cytokine release in patient-derived PBMCs. We compared a cohort of 16 donors, including healthy controls ($n = 3$) and patients with RA ($n = 2$), SLE ($n = 3$), ITP ($n = 2$), SjD ($n = 3$), and multiple myeloma ($n = 3$). Baseline E:T ratios varied by indication; multiple myeloma samples exhibited consistently higher E:T ratios, whereas healthy donor and SLE samples were characterized by lower ratios (Figure 4A).

In 96-hour TDCC assays, gamgertamig mediated potent depletion of $CD20^+$ B cells across all donor cohorts (Figure 4B). The calculated $EC_{50}$ for depletion remained consistent across all indications, ranging between 2 nM and 5 nM. Notably, baseline E:T ratio did not significantly correlate with cytotoxic potency ($EC_{50}$) or maximal efficacy ($Y_{max}$), suggesting that gamgertamig maintains robust activity even in immune environments with lower effector cell density (Supplementary Figure S5).

We further evaluated whether cytokine induction profiles varied across patient populations by calculating the fold change in IFN-γ, TNF-α, and IL-6 secretion relative to monovalent CD3

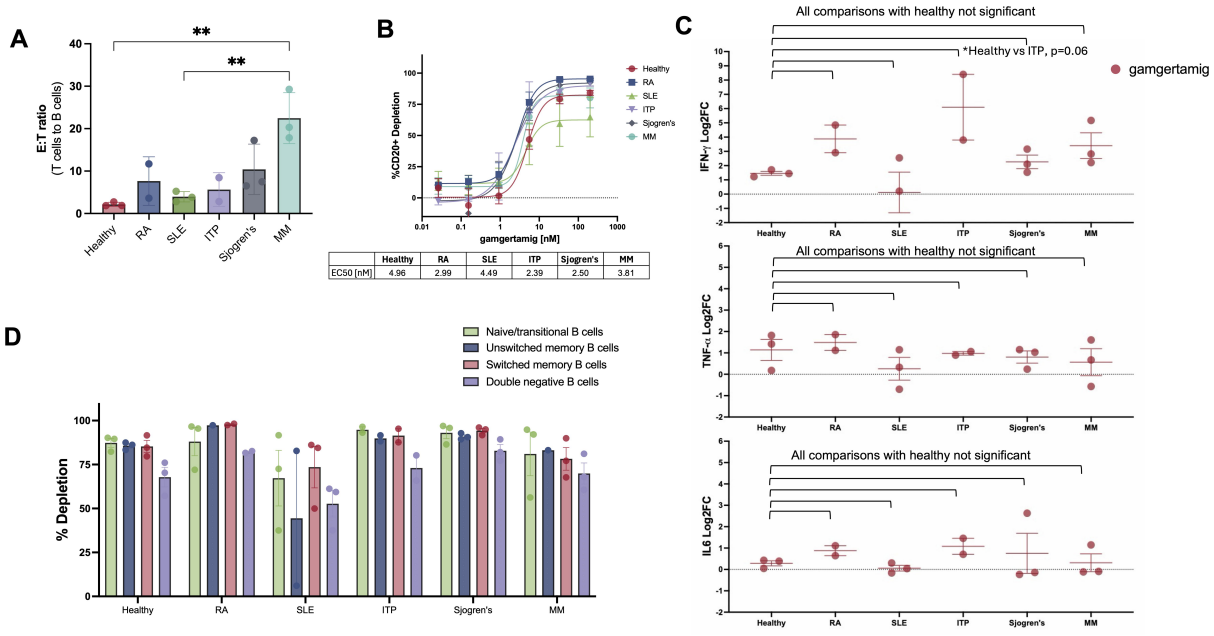


**Figure 4.** Gamgertamig induces consistent B cell depletion across autoimmune and myeloma PBMC samples. Cytotoxicity and cytokine release were measured after a 96-hour co-culture of test articles and 16 different PBMC donors: 3 healthy, 2 patients with rheumatoid arthritis (RA), 3 patients with systemic lupus erythematosus (SLE), 2 patients with immune thrombocytopenia (ITP), 3 patients with Sjögren's disease, and 3 patients with multiple myeloma (MM). Live $CD20^+$B cells and B cell subsets were counted via flow cytometry. Cytotoxicity was calculated using the ratio of live $CD3^-CD20^+$B cells or respective B cell subset in treated samples versus counts from untreated samples. Data from donors were averaged for each indication, respectively. (A) Baseline T cell ($CD3^+CD20^-$) and B cell ($CD3^-CD20^+$) counts were used to calculate average E:T ratio (effector – T cells to targets – B cells) for each indication group. (B) $CD20^+$ B cell depletion was measured in all autoimmune groups, and the curve was fit with a non-linear agonist vs response four parameter fit via GraphPad Prism. Gamgertamig shows comparable, potent depletion in all indication groups. (C) Secreted IFN-γ, TNF-α, and IL-6 cytokines were measured via ELISA from supernatant collected after 96 hours of co-culture at the 200 nM concentration. The $\log_2$fold change (Log2FC) was calculated by normalizing to the cytokine levels from the one-armed CD3 group. Statistical analysis was performed using a one-way ANOVA with multiple comparisons. No significant differences were observed between healthy controls and any autoimmune indication. A numerical trend toward higher IFN-γ levels was noted in ITP samples relative to healthy controls, although this did not reach statistical significance. (D) Percent depletion of each B cell subset in each indication group. All B cell subsets in all indications showed significant depletion.

controls. No significant differences in cytokine induction were observed between any autoimmune indication and the healthy control cohort (Figure 4C). While a numerical trend toward higher IFN-γ levels was noted in ITP patients relative to healthy donors, this comparison did not reach statistical significance and likely reflects the small sample size of that specific subset. Importantly, all other pairwise comparisons between healthy controls and autoimmune indications were non-significant, suggesting that the cytokine release profile is consistent across different disease states. This uniformity supports the use of cytokine data from healthy donors as a reliable surrogate for predicting the baseline inflammatory potential of gamgertamig in broader patient populations.

Finally, we assessed whether specific B cell subsets exhibited differential susceptibility to depletion across disease states. Most subsets across all indications achieved > 80% depletion (Figure 4D). While double-negative ($CD27^-/IgD^-$) B cells showed slightly lower maximal killing across all groups, there were no significant trends suggesting that specific subsets within any indication were uniquely resistant to gamgertamig. Despite some donor-to-donor variability, particularly within the SLE cohort, these data demonstrate that the pan-B cell depletion profile of gamgertamig is highly conserved across diverse autoimmune and malignant conditions.

### *Gamgertamig demonstrates dose-dependent antitumor efficacy in BCMA$^+$ xenograft models*

The antitumor efficacy of gamgertamig was assessed in two independent xenograft models of multiple myeloma in human PBMC-reconstituted B-NDG mice using the BCMA$^+$ cell lines NCI-H929 and MM.1S. Published QuantiBRITE analysis has characterized NCI-H929 as a high-BCMA-density myeloma cell line and MM.1S as an intermediate-BCMA-density model,[20] providing context for evaluating gamgertamig activity across models with distinct levels of BCMA expression.

In the NCI-H929 model, mice were inoculated subcutaneously (SC) with tumor cells and engrafted with human PBMCs before treatment. Animals received two SC doses of gamgertamig (0.04, 0.2, or 1 mg/kg, Q5D × 2) or a non-targeting control bispecific antibody (anti-KLH × CD3, 1 mg/kg). The control bispecific had minimal effect on tumor growth (tumor inhibition rate [TIR] = 8%), whereas gamgertamig produced dose-dependent tumor growth inhibition with mean TIRs of 47%, 50%, and 95%, respectively (Figure 5A). In addition to growth inhibition, tumor regressions below the starting volume were observed in 1/10, 3/10, and 6/10 animals at these doses. No significant body-weight loss was observed. One mouse in the vehicle group and two in the control bispecific group died (days 15–17), likely due to graft-versus-host disease (GVHD), a known complication of human PBMC-reconstituted immunodeficient mouse models caused by activation of human T cells against murine tissues.[21] No gamgertamig-related deaths occurred.

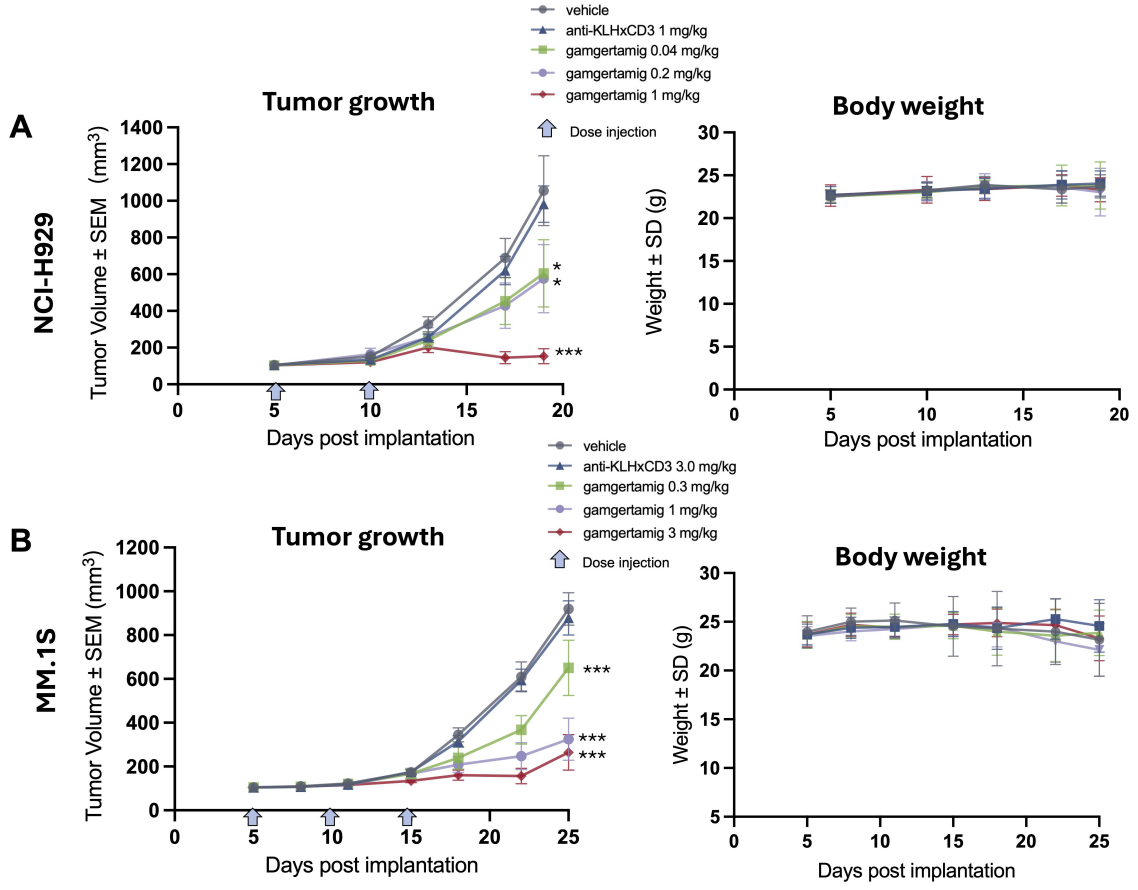


**Figure 5.** Gamgertamig demonstrates dose-dependent antitumor activity in myeloma xenograft models. Anti-tumor activity of gamgertamig was assessed in NCI-H929 and MM.1S mouse xenograft models. B-NDG mice were injected with NCI-H929 or MM.1S cells, followed by injection of human PBMCs. Gamgertamig, anti-KLH×CD3 negative control, or vehicle was injected subcutaneously after tumors reached 100mm$^3$. (A) All doses of gamgertamig demonstrated tumor control of NCI-H929 cells and did not impact body weight. The top dose of 1mg/kg prevented tumor growth. (B) All doses of Gamgertamig demonstrated tumor growth inhibition of MM.1S and did not impact body weight. Tumor inhibition rate is calculated as ([TIR]%=100 - ($T_{Dlast}$-$T_{D5}$)/($C_{Dlast}$-$C_{D5}$)*100) where T is a treated group and C is the control group and values represent tumor volume means on the last day of the study (Dlast) or day 5 (D5). Statistical comparisons of tumor volume between each gamgertamig-treated group and the vehicle group were performed at the end of each experiment—day 19 for NCI-H929 and day 25 for MM.1S—using a two-sided Mann–Whitney test. * $p < 0.05$ and *** $p < 0.001$ versus vehicle.

In the MM.1S model, mice were treated with gamgertamig (0.3, 1, or 3 mg/kg, Q5D × 3) or anti-KLH × CD3 (3 mg/kg) after tumors reached ~100 $mm^3$. The control bispecific showed minimal activity (TIR = 5%), while gamgertamig inhibited tumor growth in a dose-dependent manner with TIRs of 33%, 73%, and 80%, respectively (Figure 5B). Tumor regressions below starting volume occurred in 4/10 and 3/10 animals in the 1 mg/kg and 3 mg/kg groups, respectively. A single death (day 21) occurred in the 0.3 mg/kg group, attributed to GVHD; all other gamgertamig-treated mice tolerated therapy without body-weight loss, clinical or behavioral abnormalities. Tumor volumes were compared after the last day in both studies to determine significant differences compared to vehicle (Supplementary Figure S6).

Together, these studies demonstrate that gamgertamig elicits potent, dose-dependent antitumor activity in human PBMC-reconstituted xenograft models of multiple myeloma, with up to 95% tumor inhibition and no overt toxicity, as evidenced by stable body weight, across both $BCMA^+$ cell lines.

## *Gamgertamig demonstrates prolonged half-life and sustained B cell and plasma-cell depletion in rhesus monkeys*

Gamgertamig was evaluated in a single-dose pilot study and a 4-week repeat-dose study in rhesus monkeys to assess PK and pharmacodynamic (PD) effects on B cell and plasma-cell populations. Animals received SC or intravenous (IV) doses of gamgertamig or vehicle once on day 0 or weekly for four weeks. In the single dose PK study, serum antibody concentrations were monitored throughout the study and in the repeat dose study, immune cells were counted via peripheral blood draw and bone marrow aspirates.

Because human IgG4 exhibits strong binding to rhesus FcRn, gamgertamig was expected to display an extended serum half-life, characteristic of antibodies with intact FcRn recycling. Consistent with this, gamgertamig was detectable in serum for the full monitoring period, up to day 39 for doses of 0.15 mg/kg (SC), 0.5 mg/kg (SC), and 0.5 mg/kg (IV), and up to day 60 for 1.5 mg/kg (SC) (Figure 6A). The mean terminal half-life ranged from 140 to 185 hours for SC dosing and was 147 hours following IV administration, values that are broadly consistent with reported nonhuman-primate experience for Fc-containing human IgG4 antibodies and supportive of preserved Fc-dependent serum persistence.[22]

To evaluate PD activity in the repeat-dose study, peripheral blood B cell counts were measured periodically through day 57. B cell levels declined sharply after the first dose, falling from baseline values of 600–850 cells/μL to <100 cells/μL by day 14, and remained suppressed until day 43, which was multiple weeks after dosing had concluded (Figure 6B). Dose-dependent recovery was observed, where B cells reached and even surpassed the initial levels in the lowest 0.5 mg/kg dose while counts from the 1.5 mg/kg and 4.5 mg/kg groups recovered slower. AUC analysis of circulating $CD20^+$ cells showed significant reductions in total B cell exposure over time at 1.5 mg/kg and 4.5 mg/kg, but not at 0.5 mg/kg. Plasma-cell frequencies were assessed from bone-marrow smears collected on days 30 and 58. Compared with vehicle controls, all gamgertamig dose groups exhibited reduced plasma-cell percentages. Statistically significant reductions were observed for 0.5 mg/kg and 4.5 mg/kg dose levels at day 30 and for all dose levels at day 58. At 0.5 mg/kg, a partial recovery trend was observed by day 58, whereas plasma-cell levels remained suppressed at other dose levels (Figure 6C).

Animal body weights were monitored throughout the study as a clinical indicator of general well-being. No significant changes in body weight were observed during the active dosing period from day 0 to day 28 across any treatment group (Figure 6D). During the subsequent recovery phase, the 1.5 mg/kg and 4.5 mg/kg dose groups exhibited modest declines in mean body weight. However, maximum percent body-weight loss was not significantly different from vehicle for any gamgertamig dose group. The 0.5 mg/kg group remained essentially unaffected, and weights in the 1.5 mg/kg cohort began trending back toward pre-treatment levels by the end of the monitoring period. All animals survived the study to their scheduled necropsy.

Overall, gamgertamig was well tolerated at lower doses and exhibited a prolonged half-life (>5 days), with sustained PD activity. Notably, the molecule produced sustained depletion of circulating B cells and bone-marrow plasma cells in rhesus monkeys, supporting its potential to target both antibody-secreting and non-secreting lineages in autoimmune disease.

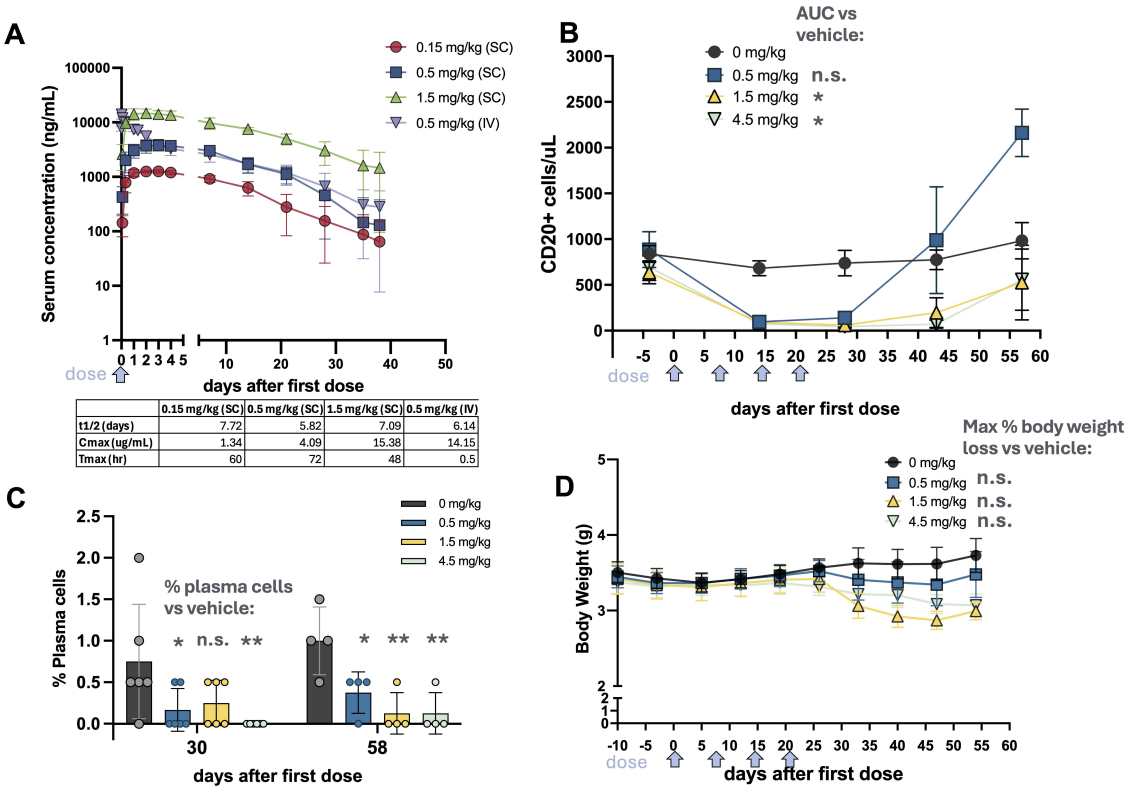


| | 0.15 mg/kg (SC) | 0.5 mg/kg (SC) | 1.5 mg/kg (SC) | 0.5 mg/kg (IV) |
|---|---|---|---|---|
| t1/2 (days) | 7.72 | 5.82 | 7.09 | 6.14 |
| Cmax (ug/mL) | 1.34 | 4.09 | 15.38 | 14.15 |
| Tmax (hr) | 60 | 72 | 48 | 0.5 |

**Figure 6.** Gamgertamig exhibits favorable pharmacokinetics and sustained B cell depletion in nonhuman primates. (A) Gamgertamig was injected subcutaneously (SC) or intravenously (IV) at a single dose, and the serum concentration was measured through bleeds over 38 days. All doses demonstrated favorable pK with $t_{1/2}$ above 5 days and detectable antibody titers through the end of the study. (B) Gamgertamig was injected SC in a repeated dose PD study. B cells were significantly reduced by day 14 but then recovered over time in all dose levels. Statistical comparisons were performed using individual animal AUC values calculated from $CD20^{+}$cells/μL over time, with ordinary one-way ANOVA and Dunnett's multiple comparisons test versus vehicle; adjusted *p* values were 0.8586 for 0.5 mg/kg, 0.0147 for 1.5 mg/kg, and 0.0110 for 4.5 mg/kg. (C) The percentage of plasma cells from bone marrow smears was calculated 30 and 58 days after the first injection. Evidence of plasma cell depletion in comparison to the vehicle group (0 mg/kg) was observed in all dose levels. For bone marrow plasma-cell percentages, statistical comparisons were performed separately at each timepoint using ordinary one-way ANOVA with Dunnett's multiple comparisons test versus vehicle. (D) Body weights were measured throughout the repeated dose PD study. Moderate body weight decreases were observed in the recovery period starting at day 28 for the 1.5 mg/kg and 4.5 mg/kg doses. Maximum percent body-weight loss from baseline was calculated for each animal and compared across groups using ordinary one-way ANOVA with Dunnett's multiple comparisons test versus vehicle.

## Discussion

B cell depletion is a cornerstone of therapy for antibody-mediated autoimmune diseases. While anti-CD19 and anti-CD20 therapies are effective, they spare LLPCs that drive autoantibody production and disease persistence.[1,23,24] Targeting BCMA has the potential to eliminate both terminally differentiated plasma cells and broader autoreactive B-cell compartments.[12,16,25] This broader expression pattern has only recently been appreciated, with the first evidence of a BCMA TCE facilitating depletion of $CD19^{+}$ B cells in clinical practice reported at the end of 2023.[14] Our studies demonstrate that gamgertamig, a BCMA×CD3 TCE, achieves potent cytotoxicity across antigen densities, B cell lineages, and patient populations, supporting its development in oncology and autoimmune disease. These findings provide a framework for evaluating how bispecific antibody design parameters influence functional activity in BCMA-directed TCEs.

Teclistamab, a clinically approved BCMA×CD3 bispecific antibody for relapsed or refractory multiple myeloma, represents an important benchmark for BCMA-directed T-cell engagement. The teclistamab analog was included as a clinically validated reference molecule to contextualize gamgertamig's activity rather than to establish superiority. Like teclistamab, gamgertamig is an IgG-based BCMA×CD3

TCE with an SP34-derived CD3-binding arm. However, gamgertamig binds CD3 with ~3-fold lower affinity while maintaining high-affinity BCMA binding, resulting in a > 50-fold BCMA-to-CD3 affinity bias intended to favor target-dependent T-cell activation.[26,27] SP34-derived and other N-terminal CD3ε-directed binders have been associated with potential polyreactivity in prior reports.[28] These class-level considerations cannot be excluded for the gamgertamig CD3 arm based on the present studies. However, SP34-derived CD3-binding arms are present in multiple clinically approved TCEs, including teclistamab,[16] talquetamab,[29] tarlatamab,[30] and glofitamab,[31] providing clinical precedent for this CD3-binding class. Gamgertamig also incorporates an affinity-attenuated CD3 arm, and its half-life in rhesus monkeys is consistent with the absence of a major nonspecific clearance liability. Together with target-dependent activity in functional assays, these findings support the suitability of the selected CD3 arm in the gamgertamig bispecific format.

Soluble BCMA may compete with membrane-bound BCMA for engagement by BCMA-directed TCEs, particularly in multiple myeloma, where soluble BCMA levels can be elevated. Although soluble BCMA spike-in studies were not performed with gamgertamig, published teclistamab data showing preserved cytotoxicity and T-cell activation in the presence of soluble BCMA provide supportive context.[32] Together with the comparable or higher BCMA affinity of gamgertamig relative to the teclistamab analog, these findings suggest that soluble BCMA may not fully abrogate gamgertamig activity, although direct studies will be needed to confirm this. Additionally, soluble BCMA levels reported in autoimmune diseases such as SLE[33] are substantially lower than levels typically reported in newly diagnosed or relapsed multiple myeloma,[34] where BCMA-directed TCEs have demonstrated clinical efficacy at tolerable dose levels.[16] This suggests that soluble BCMA-mediated antigen sink may be less likely to preclude desired function in autoimmune settings.

In comparative assays, gamgertamig demonstrated comparable maximal cytotoxicity to the teclistamab analog and trended toward lower cytokine release; however, these differences did not reach statistical significance and therefore do not establish functional superiority in vitro. Nevertheless, full dose-response analyses confirmed that affinity attenuation did not interfere with functional efficacy and may have clinical relevance if reduced CD3 engagement contributes to controlled T-cell activation in vivo. Clinically reported relapsed/refractory multiple myeloma data show predominantly low-grade cytokine release syndrome (CRS) with gamgertamig at the expansion dose, with grade 1 and grade 2 CRS in 61% and 8% of patients, respectively, and no grade ≥ 3 CRS.[35] In the MajesTEC-1 trial, teclistamab was associated with grade 1, grade 2, and grade 3 CRS in 50%, 21%, and 0.6% of patients, respectively.[36] These cross-trial data suggest broadly comparable CRS profiles, with numerically lower grade ≥ 2 CRS reported for gamgertamig, but are limited by differences in study design, patient populations, disease burden, dosing, and CRS management. Inflammatory adverse events, including cytokine release syndrome and neurotoxicity, may also be lower in autoimmune disease than in multiple myeloma due to lower antigen load and reduced overall B cell burden.[37–40]

A pivotal finding is the potent activity of gamgertamig against primary human B cells despite surface BCMA levels often remaining below the detection limit of conventional flow cytometry. This is consistent with recent high-sensitivity analyses and clinical observations showing that BCMA expression and BCMA-directed depletion can extend into $CD19^+$ B cell compartments.[15] These data suggest that trace BCMA expression is sufficient to trigger T cell–mediated cytotoxicity at physiologically relevant E:T ratios. Although high-sensitivity BCMA quantification was not performed on each depleted subset, the lack of appreciable activity with the one-armed CD3 control and the significant reduction of depletion in the presence of a BCMA-blocking antibody support BCMA-dependent, rather than nonspecific, depletion. Activity was consistent across a 16-donor cohort including healthy controls, patients with autoimmune diseases (SLE, RA, ITP, and SjD), and patients with multiple myeloma. Cytotoxic potency ($EC_{50}$) was independent of baseline E:T ratio, indicating maintained efficacy even in lymphopenic environments or tissues with low T cell density. This observation has implications for target selection in bispecific antibody design, suggesting that even low levels of antigen expression may be sufficient to support T cell–mediated cytotoxicity.

The translational relevance of gamgertamig is further supported by our in vivo findings. In xenograft models, the ability of the molecule to control rapidly proliferating myeloma cells confirms its robust intrinsic potency. In rhesus monkeys, gamgertamig exhibited a favorable PK profile with a half-life exceeding 5 days across all dose levels. This was accompanied by sustained depletion of both circulating

B cells and bone-marrow plasma cells. The reduction of plasma cells in the bone marrow is particularly significant because this compartment serves as a sanctuary for the LLPCs that drive autoantibody persistence. In lower doses, these effects were achieved without weight loss or systemic toxicity in a translationally relevant species.

In conclusion, gamgertamig represents a scalable, off-the-shelf alternative to cellular therapies for B cell–mediated diseases. By combining deep plasma-cell depletion with a consistent functional profile across preclinical systems, gamgertamig demonstrates robust activity in both oncological and autoimmune contexts. Clinical development is ongoing across multiple oncological and autoimmune indications, underscoring the translational relevance of these findings. Notably, early clinical observations suggest activity of gamgertamig in refractory autoimmune settings, including patients who have relapsed following prior cellular therapies.[10] Overall, these findings highlight key considerations for the design and evaluation of BCMA-directed bispecific antibodies and support the continued development of T cell–redirecting therapeutics with optimized functional profiles.

## Materials and methods

### *CD3 variant binding to Jurkat T cells*

Binding of humanized CD3 VH/VL variants to CD3-expressing Jurkat cells was assessed by flow cytometry. Cells were incubated with serially diluted antibodies at 4°C for 1 h, followed by staining with Alexa Fluor 647–conjugated goat anti-human IgG Fc secondary antibody (Jackson ImmunoResearch, Cat#109–606-170). After washing, samples were analyzed by flow cytometry (iQue, Intellicyt), and binding was quantified as mean fluorescence intensity.

### *Binding of BCMA×CD3 variants to BCMA-expressing cells*

Binding of BCMA×CD3 bispecific variants (κλ003–κλ006) to CHO cells stably expressing human or cynomolgus BCMA was evaluated by flow cytometry. Cells were incubated with serially diluted antibodies at 4°C for 1 h, followed by staining with Alexa Fluor 647–labeled goat anti-human IgG Fc secondary antibody (Jackson ImmunoResearch, Cat#109–606-170). After washing, samples were analyzed by flow cytometry, and binding was quantified as mean fluorescence intensity.

### *BCMA and CD3 affinity measurements*

Binding kinetics to human BCMA and CD3 were measured by bio-layer interferometry (Gator Plus) using anti-human IgG Fc Gen II biosensors (Gator Bio, Cat# 160,024). Sensors were exposed to 7-point serial dilutions (0.88–1111 nM) of His-tagged BCMA (Acro Biosystems, Cat# BCA-H522y) or His-tagged human CD3ε/δ heterodimer (Acro Biosystems, Cat# CDD-H52W1). Gamgertamig and anti-KLHxCD3 controls were produced in house. Teclistamab analog was purchased from MedChemExpress (Cat# HY-P99392). All binding interactions were performed in triplicate and the association and dissociation rates were fit with a 1:1 model to derive Kd values ($n = 3$).

### *Binding on cell lines*

Binding to multiple myeloma cell lines NCI-H929 (ATCC, CRL-3580), MM.1S (ATCC, CRL-2974), and RPMI 8226 (ATCC, CRM-CCL-155) was assessed by flow cytometry following incubation with titrated gamgertamig, teclistamab analog (MedChemExpress, Cat# HY-P99392) or a non-targeting control bispecific antibody (anti-KLH×CD3). EC50 values were derived from four-parameter logistic fits of mean fluorescence intensity.

### Quantification of surface BCMA expression

Parental Mino cells were sourced from ATCC (CRL-3000) and engineered to express GFP/luciferase by lentiviral integration at Sino Biological. NCI-H929 (GFP/luc) cells were sourced from ATCC (CRL-3580-GFP-LUC2). BCMA expression was quantified on Mino (GFP/luc) and NCI-H929 (GFP/luc) cells using QuantiBRITE PE beads (BD Biosciences, Cat# 340,495) according to the manufacturer's instructions. Cells were stained at saturation with phycoerythrin (PE)-conjugated anti-BCMA antibody (clone 19F2, BioLegend), and geometric MFI values were converted to PE molecules per cell using bead standards. Values were corrected for the antibody labeling ratio (1.12 PE/IgG) to calculate antibodies bound per cell (ABC).

### In vitro cytotoxicity and cytokine profiling in BCMA$^+$ target cells

TDCC assays were performed using NCI-H929 (GFP/luc) and Mino (GFP/luc) cells with varying BCMA expression. Gamgertamig, teclistamab, or a monovalent CD3 control were added in titrations starting at 25 or 50 nM. PBMCs from three healthy donors (Sanguine Biosciences) were co-cultured with target cells at a 10:1 ratio for 24–72 hours. RPMI 1640 media (Corning, Cat# 0–104-CV) with 10% HI FBS (VWR, Cat# VWR 1500–050 H) and 1% pen-strep (VWR, Cat# 45,000–653) was used for the duration of the assay. Cytotoxicity was measured by a One-Glo EX luciferase-based assay (Promega, E8110) and calculated as (treated – untreated)/untreated signal. Cytokines (TNF-α, IL-6, IFN-γ) were quantified in 48-hour supernatants using Lumit® immunoassays (Promega; IFN-γ Cat# W6041, IL-6 Cat# W6031).

### Ex vivo cytotoxicity and cytokine profiling in healthy and autoimmune PBMCs

TDCC assays were performed using PBMCs from healthy and autoimmune donors ($n$ = 16; 3 healthy, 2 RA, 3 SLE, 2 ITP, 3 SjD, 3 multiple myeloma). Human PBMCs and primary donor samples were obtained commercially from Sanguine Biosciences (San Diego, CA, USA). Samples were collected with donor consent under Institutional Review Board–approved protocols and provided to the investigators as de-identified biospecimens without protected health information. PBMCs (200,000/well) were incubated with titrated gamgertamig, teclistamab, or monovalent CD3 control (up to 200 nM) for 96 hours. Cytokines (TNF-α, IL-6, IFN-γ) were quantified in supernatants using Lumit® immunoassays (Promega). Cytotoxicity was assessed by flow cytometry as the percentage of live cells relative to untreated controls on a per-donor basis.

For blocking studies, healthy donor PBMCs from two donors were plated at 200,000 cells/well with two technical replicates per donor. Cells were pre-incubated for 1 hour with 1 μM bivalent anti-BCMA blocking antibody containing the same BCMA-binding arm as gamgertamig but lacking a CD3-binding arm, or with a bivalent anti-CD19 control antibody based on the tafasitamab binder. Both blocking antibodies were formatted as IgG1 LALA/PG molecules and produced in house. Gamgertamig, teclistamab analog, or one-armed CD3 control was then added at 100 nM or 20 nM, and cultures were incubated for 72 hours. B cell depletion was assessed by flow cytometric enumeration of live CD20$^+$ cells and calculated as percent lysis relative to untreated wells.

### Mice

Female B-NDG mice, 7 weeks of age, were obtained from Biocytogen Pharmaceuticals (Jiangsu) Co., Ltd. and housed under specific pathogen-free conditions at Shanghai Institute of Materia Medica, Chinese Academy of Sciences. The animal production license number was SCXK (Su) 2016–0004. Animal use and welfare procedures were conducted in accordance with institutional animal care procedures and Association for Assessment and Accreditation of Laboratory Animal Care International (AAALAC) standards. Animals were monitored daily for general health, mortality, behavior, body weight, appearance, and clinical signs.

### In vivo antitumor efficacy

In vivo efficacy was evaluated in human PBMC-reconstituted subcutaneous xenograft models using female B-NDG mice. For the NCI-H929 model, mice were inoculated subcutaneously with NCI-H929 cells ($2 \times 10^6$ cells/mouse, 1:1 Matrigel), followed by intravenous injection of human PBMCs ($1 \times 10^7$ cells/mouse). For the MM.1S model, mice were inoculated subcutaneously with MM.1S cells ($6 \times 10^6$ cells/mouse), followed by intravenous injection of human PBMCs ($1 \times 10^7$ cells/mouse).

When tumors reached approximately 100 $mm^3$, mice were randomized by tumor volume and assigned to treatment groups. In the NCI-H929 study, mice received vehicle, anti-KLH×CD3 isotype control at 1 mg/kg, or gamgertamig at 0.04, 0.2, or 1 mg/kg by subcutaneous injection every 5 days for two doses. In the MM.1S study, mice received vehicle, anti-KLH×CD3 isotype control at 3 mg/kg, or gamgertamig at 0.3, 1, or 3 mg/kg by subcutaneous injection every 5 days for three doses. Each treatment group included 10 mice at study initiation.

Tumor dimensions were measured twice weekly using calipers, and tumor volume was calculated as $0.5 \times \text{length} \times \text{width}^2$. Antitumor activity was assessed by tumor growth inhibition and tumor regression. Partial regression was defined as tumor volume smaller than baseline volume at treatment initiation, and complete regression was defined as no detectable tumor. Body weight and clinical observations were monitored during the study. At study termination, animals were euthanized under $CO_2$ anesthesia, and tumors were collected and weighed. Statistical comparisons of tumor volume or tumor weight between groups were performed using a two-tailed Student's t-test unless otherwise specified, with $p < 0.05$ considered statistically significant.

### Non-human primates

Rhesus monkeys (Macaca mulatta) were obtained from Yunnan Jinjiekang Biotechnology Co., Ltd. and housed at Jiangsu Tripod Preclinical Research Laboratories Co., Ltd., an AAALAC-accredited facility. The animal production license number was SCXK (Yunnan) 2018–0002, and the laboratory animal use license number was SYXK (Su) 2020–0007. The animal protocol was reviewed and approved by the Institutional Animal Care and Use Committee of Jiangsu Tripod Preclinical Research Laboratories Co., Ltd. before animal use; the approved animal protocol number was AP-2096–380. The study was conducted under Good Laboratory Practice conditions, except for the binding activity analysis, and in accordance with applicable NMPA and ICH guidelines.

### Nonhuman primate PK and PD study

A single-dose pharmacokinetic study of gamgertamig was conducted in 24 rhesus monkeys randomized into four groups of six animals each, with three males and three females per group. Animals received a single subcutaneous dose of gamgertamig at 0.15, 0.5, or 1.5 mg/kg or a single 30-min intravenous infusion at 0.5 mg/kg. Serial blood samples were collected through day 38. Serum gamgertamig concentrations were measured by ELISA and analyzed by noncompartmental methods.

A 4-week repeat-dose pharmacology and toxicity study of gamgertamig was conducted in rhesus monkeys with a 4-week recovery period. Forty animals, 20 males and 20 females, approximately 2.8–4.5 years of age at dosing initiation, were stratified by sex and body weight and randomized into four groups of 10 animals each, with 5 males and 5 females per group. Animals received vehicle or gamgertamig at 0.5, 1.5, or 4.5 mg/kg by subcutaneous injection once weekly for 4 consecutive weeks, for a total of four doses. The dosing volume was 1 mL/kg, and the dose was calculated based on the most recent scheduled body weight. The subcutaneous route was selected to match the intended clinical route of administration. Rhesus monkeys were selected as the pharmacologically relevant nonclinical species based on cross-reactive binding of gamgertamig to rhesus BCMA and CD3 and preliminary evidence of pharmacodynamic activity in rhesus monkeys.

Clinical observations were performed at least twice daily, with detailed observations performed weekly. Pharmacokinetic, pharmacodynamic, safety pharmacology, clinical pathology, immunogenicity, local

tolerability, and pathology assessments were performed according to the study protocol. Peripheral $CD20^+$ B cells were quantified by flow cytometry, and plasma cells were assessed in bone marrow smears at necropsy.

At the end of the dosing period, animals not assigned to recovery were euthanized and necropsied on Day 30. Recovery animals, consisting of two males and two females per group, were euthanized and necropsied on Day 58 after a 4-week treatment-free recovery period. Euthanasia was performed under anesthesia in accordance with institutional procedures and AVMA principles.

## Acknowledgments

This study was conducted by employees of Ouro Medicines and Keymed Biosciences and supported by these organizations. ChatGPT (OpenAI, GPT-5.3) was used to assist with editing and revision of the manuscript text.

## Author contributions

CRediT: **Jamie Thomas:** Investigation, Writing – original draft; **Gang Xu:** Project administration; **Hannah Lock:** Investigation, Writing – original draft; **Qin Song:** Data curation, Methodology, Project administration; **Yumei Yin:** Investigation; **Wanying Luo:** Investigation; **Kyu Hong:** Investigation; **Liguang Lou:** Investigation; **Changyu Wang:** Conceptualization, Project administration; **Leslie Chinn:** Writing – review & editing; **Neelufar Mozaffarian:** Conceptualization, Supervision, Writing – review & editing; **Jaideep Dudani:** Supervision, Writing – review & editing; **Paul Bessette:** Methodology, Writing – review & editing; **Charlie Zhou:** Conceptualization, Supervision, Writing – review & editing; **Ruth Lan:** Methodology, Supervision, Writing – review & editing; **Bo Chen:** Project administration, Supervision; **Nishant Mehta:** Conceptualization, Methodology, Project administration, Supervision, Writing – original draft, Writing – review & editing.

## Disclosure statement

JT, HL, KH, LC, NM, JD, PB, CZ, RL, and NM are employees of Ouro Medicines and may hold equity in the company. GX, QS, YY, WL, CW, and BW are employees of Keymed Biosciences and may hold equity in the company. No other competing financial interests were declared.

## Funding

The author(s) reported there is no funding associated with the work featured in this article.

## Data availability statement

The data that support the findings of this study are available from the corresponding author, NM, upon reasonable request.

## References

1. Edwards JC, Szczepański L, Szechiński J, Filipowicz-Sosnowska A, Emery P, Close DR, Stevens RM, Shaw T. Efficacy of B-Cell–targeted therapy with rituximab in patients with rheumatoid arthritis. N Engl J Med. 2024;350:2572–2581. doi: 10.1056/NEJMoa032534.
2. Furie R, Rovin BH, Houssiau F, Malvar A, Teng YKO, Contreras G, Amoura Z, Yu X, Mok C-C, Santiago MB, Saxena A. Two-year, randomized, controlled trial of belimumab in lupus nephritis. N Engl J Med. 2020;383 (12):1117–1128. doi: 10.1056/NEJMoa2001180.
3. Müller F, Hagen M, Wirsching A, Kharboutli S, Aigner M, Völkl S, Kretschmann S, Tascilar K, Taubmann J, Bucci L, et al. CD19 CAR-T cells for treatment-refractory autoimmune diseases: the phase 1/2 CASTLE basket trial. Nat Med. 2026;32(3):1142–1151. doi: 10.1038/s41591-025-04185-6.
4. Bucci L, Böltz S, Hagen M, Tur C, Nöthling D-M, Rothe T, Wirsching A, Auth J, Wacker J, Eckstein M, et al. BCMA T-Cell engager therapy in patients with refractory autoimmune disease. N Engl J Med. 2025;393 (15):1544–1547. doi: 10.1056/NEJMc2506740.
5. Junt T, Calzascia T, Traggiai E, da Costa AN, Gergely P, Schett G, Dörner T, Siegel RM. Defining immune reset: achieving sustained remission in autoimmune diseases. Nat Rev Immunol. 2025;25(7):528–541. doi: 10.1038/s41577-025-01141-w.

6. Mei HE, Wirries I, Frölich D, Brisslert M, Giesecke C, Grün JR, Alexander T, Schmidt S, Luda K, Kühl AA, et al. A unique population of IgG-expressing plasma cells lacking CD19 is enriched in human bone marrow. Blood. 2015;125(11):1739–1748. doi: 10.1182/blood-2014-02-555169.
7. Halliley JL, Tipton C, Liesveld J, Rosenberg A, Darce J, Gregoretti I, Popova L, Kaminiski D, Fucile C, Albizua I, et al. Long-lived plasma cells are contained within the CD19−CD38hiCD138+ subset in human bone marrow. Immunity. 2015;43(1):132–145. doi: 10.1016/j.immuni.2015.06.016.
8. Brynjolfsson SF, Mohaddes M, Kärrholm J, Wick M-J. Long-lived plasma cells in human bone marrow can be either CD19+ or CD19−. Blood Adv. 2017;1(13):835–838. doi: 10.1182/bloodadvances.2017004481.
9. Müller F, Wirsching A, Hagen M, Völkl S, Tur C, Raimondo MG, Taubmann J, Bucci L, Zhang L, Kretschmann S, et al. BCMA CAR T cells in a patient with relapsing idiopathic inflammatory myositis after initial and repeat therapy with CD19 CAR T cells. Nat Med. 2025;31(6):1793–1797. doi: 10.1038/s41591-025-03718-3.
10. Zhang L, Gao Z, Pan H, Li R, Fang L, Li W, Zhao J, Yu X, Kuang Z, Nie N, et al. BCMA-Targeted T-Cell engager for autoimmune hemolytic anemia after CD19 CAR T-Cell therapy. N Engl J Med. 2025;392(22):2282–2284. doi: 10.1056/NEJMc2502297.
11. Chen Y, Xu Y, Li H, Sun T, Cao X, Wang Y, Xue F, Liu W, Liu X, Dong H, et al. A novel anti-CD38 monoclonal antibody for treating immune thrombocytopenia. N Engl J Med. 2024;390(23):2178–2190. doi: 10.1056/NEJMoa2400409.
12. O'Connor BP, Raman VS, Erickson LD, Cook WJ, Weaver LK, Ahonen C, Lin L-L, Mantchev GT, Bram RJ, Noelle RJ. BCMA is essential for the survival of long-lived bone marrow plasma cells. J Exp Med. 2004;199(1):91–98. doi: 10.1084/jem.20031330.
13. Cornelis R, Chang H-D, Radbruch A. Keeping up with the stress of antibody production: BAFF and APRIL maintain memory plasma cells. Curr Opin Immunol. 2021;71:97–102. doi: 10.1016/j.coi.2021.06.012.
14. Frerichs KA, Verkleij CPM, Mateos MV, Martin TG, Rodriguez C, Nooka A, Banerjee A, Chastain K, Perales-Puchalt A, Stephenson T, et al. Teclistamab impairs humoral immunity in patients with heavily pretreated myeloma: importance of immunoglobulin supplementation. Blood Adv. 2024;8(1):194–206. doi: 10.1182/bloodadvances.2023011658.
15. Jelinek T, Zihala D, Zabaleta A, Kostopoulos IV, Soucek O, Venglar O, Moreno C, Fotiou D, Radova E, Tamariz-Amador LE, et al. Selective B-cell subset depletion underlies increased infection risk in patients with MM treated with anti-BCMA vs anti-GPRC5D bsAbs. Blood. 2026;147(10):1070–1082. doi: 10.1182/blood.2025029572.
16. Moreau P, Garfall AL, van de Donk NWCJ, Nahi H, San-Miguel JF, Oriol A, Nooka AK, Martin T, Rosinol L, Chari A, et al. Teclistamab in relapsed or refractory multiple myeloma. N Engl J Med. 2022;387(6):495–505. doi: 10.1056/NEJMoa2203478.
17. Chen B, Xu G, Wang Y; Keymed Biosciences Co., Ltd., assignee. Development and application of t-cell engager therapeutic agent. International patent publication WO2022117045A1. 2022 June 9.
18. Ota M, Nagafuchi Y, Hatano H, Ishigaki K, Terao C, Takeshima Y, Yanaoka H, Kobayashi S, Okubo M, Shirai H, et al. Dynamic landscape of immune cell-specific gene regulation in immune-mediated diseases. Cell. 2021;184(11):3006–3021.e17. doi: 10.1016/j.cell.2021.03.056.
19. Alexander T, Krönke J, Cheng Q, Keller U, Krönke G. Teclistamab-induced remission in refractory systemic lupus erythematosus. N Engl J Med. 2024;391(9):864–866. doi: 10.1056/NEJMc2407150.
20. Bluhm J, Kieback E, Marino SF, Oden F, Westermann J, Chmielewski M, Abken H, Uckert W, Höpken UE, Rehm A. CAR T cells with enhanced sensitivity to B cell maturation antigen for the targeting of B cell non-Hodgkin's lymphoma and multiple myeloma. Mol Ther. 2018;26(8):1906–1920. doi: 10.1016/j.ymthe.2018.06.012.
21. Kametani Y, Ito R, Manabe Y, Kulski JK, Seki T, Ishimoto H, Shiina T. PBMC-engrafted humanized mice models for evaluating immune-related and anticancer drug delivery systems. Front Mol Biosci. 2024;11. doi: 10.3389/fmolb.2024.1447315.
22. Datta-Mannan A, Chow C-K, Dickinson C, Driver D, Lu J, Witcher DR, Wroblewski VJ. FcRn affinity-pharmacokinetic relationship of five human IgG4 antibodies engineered for improved in vitro FcRn binding properties in cynomolgus monkeys. Drug Metab Dispos. 2012;40(8):1545–1555. doi: 10.1124/dmd.112.045864.
23. Navarra SV, Guzmán RM, Gallacher AE, Hall S, Levy RA, Jimenez RE, Li EKM, Thomas M, Kim H-Y, León MG, et al. Efficacy and safety of belimumab in patients with active systemic lupus erythematosus: a randomised, placebo-controlled, phase 3 trial. Lancet. 2011;377(9767):721–731. doi: 10.1016/S0140-6736(10)61354-2.
24. Mougiakakos D, Krönke G, Völkl S, Kretschmann S, Aigner M, Kharboutli S, Böltz S, Manger B, Mackensen A, Schett G. CD19-targeted CAR T cells in refractory systemic lupus erythematosus. N Engl J Med. 2021;385(6):567–569. doi: 10.1056/NEJMc2107725.
25. Bossen C, Schneider PB. BAFF, APRIL and their receptors: structure, function and signaling. Semin Immunol. 2006;18(5):263–275. doi: 10.1016/j.smim.2006.04.006.
26. Mandikian D, Takahashi N, Lo AA, Li J, Eastham-Anderson J, Slaga D, Ho J, Hristopoulos M, Clark R, Totpal K, et al. Relative target affinities of T-Cell–dependent bispecific antibodies determine biodistribution in a solid tumor mouse model. Mol Cancer Ther. 2018;17:776–785. doi: 10.1158/1535-7163.MCT-17-0657.

27. Staflin K, Zuch de Zafra CL, Schutt LK, Clark V, Zhong F, Hristopoulos M, Clark R, Li J, Mathieu M, Chen X, et al. Target arm affinities determine preclinical efficacy and safety of anti-HER2/CD3 bispecific antibody. JCI Insight. 2020;5(7):133757. doi: 10.1172/jci.insight.133757.
28. Liu CY, Ahonen CL, Brown ME, Zhou L, Welin M, Krauland EM, Pejchal R, Widboom PF, Battles MB. Structure-based engineering of a novel CD3ε-targeting antibody for reduced polyreactivity. mAbs. 2023;15 (1):2189974. doi: 10.1080/19420862.2023.2189974.
29. Chari A, Minnema MC, Berdeja JG, Oriol A, van de Donk NWCJ, Rodríguez-Otero P, Askari E, Mateos M-V, Costa LJ, Caers J, et al. Talquetamab, a T-Cell–Redirecting GPRC5D bispecific antibody for multiple myeloma. N Engl J Med. 2022;387(24):2232–2244. doi: 10.1056/NEJMoa2204591.
30. Ahn M-J, Cho BC, Felip E, Korantzis I, Ohashi K, Majem M, Juan-Vidal O, Handzhiev S, Izumi H, Lee J-S, et al. Tarlatamab for Patients with Previously Treated Small-Cell Lung Cancer. N Engl J Med. 2023;389 (22):2063–2075. doi: 10.1056/NEJMoa2307980.
31. Dickinson MJ, Carlo-Stella C, Morschhauser F, Bachy E, Corradini P, Iacoboni G, Khan C, Wróbel T, Offner F, Trněný M, et al. Glofitamab for Relapsed or Refractory Diffuse Large B-Cell Lymphoma. N Engl J Med. 2022;387 (24):2220–2231. doi: 10.1056/NEJMoa2206913.
32. Pillarisetti K, Powers G, Luistro L, Babich A, Baldwin E, Li Y, Zhang X, Mendonça M, Majewski N, Nanjunda R, et al. Teclistamab is an active T cell–redirecting bispecific antibody against B-cell maturation antigen for multiple myeloma. Blood Adv. 2020;4(18):4538–4549. doi: 10.1182/bloodadvances.2020002393.
33. Salazar-Camarena DC, Palafox-Sánchez CA, Cruz A, Marín-Rosales M, Muñoz-Valle JF. Analysis of the receptor BCMA as a biomarker in systemic lupus erythematosus patients. Sci Rep. 2020;10(1):6236. doi: 10.1038/s41598-020-63390-0.
34. Wiedemann Á, Szita VR, Horváth R, Szederjesi A, Sebő A, Tóth AD, Masszi T, Varga G. Soluble B-cell maturation antigen as a monitoring marker for multiple myeloma. Pathol Oncol Res. 2023;29:1611171. doi: 10.3389/pore.2023.1611171.
35. Qiu L, Jing H, An G, Liu W, Wang Y, Zhou C, Mozaffarian N. OM336, a B cell maturation antigen (BCMA) targeting t cell engager antibody, demonstrates initial safety and efficacy in the treatment of relapsed/refractory multiple myeloma (r/r MM). EHA Poster, PS1740. 2025.
36. Martin TG, Mateos MV, Nooka A, Banerjee A, Kobos R, Pei L, Qi M, Verona R, Doyle M, Smit J, et al. Detailed overview of incidence and management of cytokine release syndrome observed with teclistamab in the MajesTEC-1 study of patients with relapsed/refractory multiple myeloma. Cancer. 2023;129(13):2035–2046. doi: 10.1002/cncr.34756.
37. Terstappen LW, Johnsen S, Segers-Nolten IM, Loken MR. Identification and characterization of plasma cells in normal human bone marrow by high-resolution flow cytometry. Blood. 1990;76(9):1739–1747. doi: 10.1182/blood.V76.9.1739.1739.
38. Yu T-S, Wang H-Y, Zhao Y-J, Yu Y-F, Hou Y, Liu S, Han P-P, Ni X-F, Ji X-B, Peng J, et al. Abnormalities of bone marrow B cells and plasma cells in primary immune thrombocytopenia. Blood Adv. 2021;5(20):4087–4101. doi: 10.1182/bloodadvances.2020003860.
39. Al Saleh AS, Parmar HV, Visram A, Muchtar E, Buadi FK, Go RS, Dispenzieri A, Kapoor P, Warsame R, Lacy MQ, et al. Increased bone marrow plasma-cell percentage predicts outcomes in newly diagnosed multiple myeloma patients. Clin Lymphoma Myeloma Leuk. 2020;20(9):596–601. doi: 10.1016/j.clml.2020.03.012.
40. Salmon SE, Smith BA. Immunoglobulin synthesis and total body tumor cell number in IgG multiple myeloma. J Clin Invest. 1970;49(6):1114–1121. doi: 10.1172/JCI106327.